Available online at www.sciencedirect.com
SCIENCE DIRECT®
International Journal of Solids and Structures 43 (2006) 2513–2541
INTERNATIONAL JOURNAL OF SOLIDS and STRUCTURES
www.elsevier.com/locate/ijsolstr

General mean-field homogenization schemes for viscoelastic composites containing multiple phases of coated inclusions

C. Friebel, I. Doghri *, V. Legat

Université Catholique de Louvain (UCL), CESAME Bâtiment Euler, 4 Avenue G. Lemaître, B-1348 Louvain-la-Neuve, Belgium

Available online 10 August 2005

Abstract

We consider matrix materials reinforced with multiple phases of coated inclusions. All materials are linear viscoelastic. We present general schemes for the prediction of the effective properties based on mean-field homogenization. There are four contributions in this work. First, we present a two-step homogenization procedure in a general setting which besides the usual assumptions of Eshelby-based models, does not suffer any restriction in terms of material properties, aspect ratio or orientation. Second, for a matrix reinforced with coated inclusions, we propose two general homogenization schemes, a two-step method and a two-level recursive scheme. We develop and compare the mathematical expressions obtained by the two schemes and a generalized Mori–Tanaka (M–T) model. Third, for a two-phase composite, either standalone or stemming from two-step or two-level schemes, we use a double-inclusion model based on a closed-form but non-trivial interpolation between M–T and inverse M–T estimates. Fourth, we conduct an extensive validation of the proposed schemes as well as others against experimental data and unit cell finite element simulations for a variety of viscoelastic composite materials. Under severe conditions, the proposed schemes perform much better than other existing homogenization methods.

Keywords: Homogenization; Viscoelasticity; Composites; Coatings; Multi-phase

1. Introduction

Pioneering contributions to the homogenization of linear viscoelastic composites were made by Hashin (1965, 1970) and Christensen (1969). In 1965, Hashin predicted the effective bulk modulus of two-phase

Abbreviations: D–I, double-inclusion; FE, finite element; LCT, Laplace–Carson transform; M–T, Mori–Tanaka.

* Corresponding author. Tel.: +32 10 478042/472350; fax: +32 10 472180.
E-mail addresses: friebel@mema.ucl.ac.be (C. Friebel), doghri@mema.ucl.ac.be (I. Doghri), vl@mema.ucl.ac.be (V. Legat).

0020-7683/$ - see front matter © 2005 Elsevier Ltd. All rights reserved.
doi:10.1016/j.ijsolstr.2005.06.035

viscoelastic composites. Christensen followed in 1969 with formulae for both bulk and shear complex moduli. Hashin also gave results for the shear modulus in 1970. All these models are based on the composite spheres assemblage developed by Hashin (1962) for elastic composites and make use of the well-known correspondence principle between linear elasticity and linear viscoelasticity. The major restriction in those models is that they consider macroscopically homogeneous composites, therefore they cannot handle fibrous composites for instance. Afterwards, the correspondence principle has been heavily used in order to extend any homogenization model valid in linear elasticity to linear viscoelasticity. Recently, Chandra et al. (2002) made a comparative study between various models, simple ones such as Halpin-Tsai, Tsai or Saravanos-Chamis or more elaborated ones like the Zao–Weng model (a modified Eshelby-based Mori–Tanaka). Predictions were compared to finite element (FE) calculations for long fiber reinforced composites.

All the above-mentioned models are for two-phase composites. Our *proposal* in this paper is to use a viscoelastic extension of an interpolative double-inclusion (D–I) mean-field homogenization model. In linear elasticity, the model was proposed by Lielens (1999) based on the Nemat-Nasser and Hori (1999) family of D–I models. It can be seen as a closed-form but non-trivial interpolation between the Mori–Tanaka (M–T) and inverse M–T estimates. The model works remarkably well from small to large values of inclusions' volume fractions and from low to high contrast values.

For multi-phase viscoelastic composites, Fisher and Brinson (2001) used a direct extension of M–T to three-phase composites. This extension suffers from some restrictions as Benveniste et al. (1989) demonstrated that in linear elasticity diagonal symmetry of the effective stiffness tensor is not always guaranteed when M–T is used for a multi-phase composite. In this paper, we *propose* a viscoelastic extension of a general two-step homogenization procedure used in linear elasticity by Camacho et al. (1990), Lielens (1999) and Pierard et al. (2004), and also extended to elastoplasticity by Doghri and Tinel (2005). The procedure is very generic, and besides the usual limitations of Eshelby-based models, does not suffer any restrictions in terms of material properties, number of phases, inclusions' shapes or orientations. The first step consists in the homogenization of two-phase pseudo-grains, and any suitable model (such as M–T) can be used in this step; we suggest using interpolative D–I. In the second step, homogenization of all pseudo grains is carried out with models leading to physically acceptable predictions (e.g., symmetric effective stiffness). We suggest using a simple Voigt model in this second step.

For viscoelastic composites, it is often assumed that energy losses occur at inclusions' boundary. This behavior can be studied by including an interphase between each inclusion and the matrix, resulting in coated inclusions composites. A first modeling approach is through finite element (FE) analysis, (e.g. Marra et al., 1999). A second approach is through the development of analytical or semi-analytical solutions in linear (thermo)-elasticity for special cases, mainly for a matrix reinforced with single or dilute concentrations of coated spheres or long cylinders. The composite-spheres assemblage of Hashin (1962) and the three-phase model by Christensen and Lo (1979) are at the origin of the n-layered spherical inclusion model by Herve and Zaoui (1993). The latter model treats coated particle-reinforced materials by considering a spherical particle surrounded by a layer of coating, itself surrounded by a layer of matrix, and the ensemble is embedded inside a medium whose elastic parameters are the overall (unknown) ones. Analytical formulae can be found for the bulk and shear moduli of these composites. The model was recently used by Chabert et al. (2004). The interphase parameters were always chosen to fit experimental data. For a single coated long cylinder embedded in a matrix body, Benveniste et al. (1989) computed stress and strain fields under axisymmetric and non-axisymmetric boundary conditions in linear thermo-elasticity.

A third modeling strategy in coated composites is mean-field homogenization. Several authors postulate that the composite's behavior is the same as if the interphase were a separate inclusion phase and use a direct extension of M–T to predict the overall properties. In linear thermo-elasticity, Benveniste et al. (1989) proposed a modified direct M–T model. They considered coatings as a separate phase but computed the strain concentration tensors not from M–T, but by solving in closed-form the problem of a single coated

long fiber, embedded in a matrix. Fisher and Brinson (2001) extended the Benveniste et al. (1989) scheme to viscoelastic coated composites and confronted the predictions to FE results. The predictions were not better than those obtained by a classical direct M–T extension treating the coatings as a separate phase. For coated spherical inclusions, Sarvestani (2003) uses M–T but accounts in a phase-averaging sense of the interaction between two coated particles. Cherkaoui et al. (1996) used a method similar to that of Benveniste et al. (1989) but developed a self-consistent (SC) scheme instead of M–T and proposed expressions of strain concentration tensors based on a thin layer asymptotic theory. The multi-inclusion model of Nemat-Nasser and Hori (1999) or its simpler double-inclusion version lead to the same overall stiffness predictions as a generalized M–T model. Recently, Aboutajeddine and Neale (2005) reformulated the Nemat-Nasser and Hori (1999) double-inclusion model.

For composites with coated inclusions, we are interested in methods which would work in a general setting and are not restricted to special shapes or loading conditions. Also, we would like to extend them to viscoelasticity, test them in severe conditions (e.g., high contrasts between material properties and high volume fraction of inclusions) and obtain good predictions for both storage and loss moduli. We *propose* two general mean-field homogenization strategies, a *two-step* procedure and a *two-level* recursive scheme. The two-step procedure treats coatings as a separate phase but instead of using a direct M–T extension, we virtually decompose the composite into two pseudo-grains (each containing a reinforced matrix) and homogenize it in two steps. We suggest interpolative D–I or M–T in the first step and Voigt in the second. In the two-level scheme, we first homogenize the coated inclusions (deepest level) and then the matrix reinforced with homogenized inclusions (highest level). We suggest using interpolative D–I or M–T at each level, and particularly the former at the deepest level.

The paper has the following outline. Viscoelasticity of homogeneous materials is presented in Section 2. In Section 3, the correspondence between linear elasticity and linear viscoelasticity is used to extend a two-step homogenization procedure to general multi-phase viscoelastic composites. Section 4 deals with general methodologies for the homogenization of coated composites. It discusses our proposed two-step and two-level schemes and compares their mathematical expressions to those of a direct M–T method. Section 5 explains the numerical Laplace–Carson inversion which is carried out in order to bring solutions back to the time domain. An extensive validation effort is carried out in Section 6 for numerous viscoelastic composite systems. The predictions of our proposed methods as well as those of other authors are compared against experimental data and unit cell finite element simulations. Conclusions are drawn in Section 7.

2. Response of a homogeneous material to harmonic loading

We briefly recall the mechanical response of linear viscoelastic materials to harmonic oscillations. A one-dimensional example is given to illustrate that the complex moduli—which completely characterize the material subjected to this kind of loadings—can be viewed as the LCT of the time moduli. Afterwards, the tensorial formalism will help us to stay as generic as possible in the developement of homogenization schemes of Section 3.

2.1. Complex modulus as the LCT of the time modulus

Consider a homogeneous viscoelastic specimen subjected to a uniaxial complex strain history $\varepsilon(t) = \varepsilon_0 e^{i\omega t}$ with amplitude ε_0 small enough for the material to remain in the linear regime. The corresponding stress response, detailed in Wineman and Rajagopal (2000), is given by

$$\sigma(t) = E^*(\omega)\varepsilon(t), \tag{1}$$

where $E^*(\omega) = E'(\omega) + iE''(\omega)$ is the complex modulus in tension. Its real and imaginary parts (storage and loss moduli resp.) are related to the recoverable and dissipated strain energy during the cycles, resp. Their ratio $\tan\delta(\omega) = \frac{E''(\omega)}{E'(\omega)}$ is then interpreted as a measure of the damping capacity of the material and is called the loss factor.

Moreover, if we define the LCT $\hat{f}(s)$ of a function $f(t)$ by s times its Laplace transform,

$$\hat{f}(s) = \mathscr{L}_c[f(t)](s) = s\mathscr{L}[f(t)](s) = s\int_0^\infty f(t)e^{-st}\,dt, \tag{2}$$

the complex modulus in tension appears to be the LCT of the corresponding time modulus for a particular value of the variable s:

$$E^*(\omega) = \mathscr{L}_c[E(t)](s)|_{s=i\omega}. \tag{3}$$

2.2. The 3D tensorial formalism

The three dimensional constitutive equation for a homogeneous linear viscoelastic material is often written under the integral relaxation form

$$\boldsymbol{\sigma}(t) = \boldsymbol{G}(t) : \boldsymbol{\varepsilon}(0) + \int_0^t \boldsymbol{G}(t-\tau) : \dot{\boldsymbol{\varepsilon}}(\tau)\,d\tau \quad \text{with } \boldsymbol{\varepsilon}(0) = \lim_{\substack{t\to 0\\ t>0}} \boldsymbol{\varepsilon}(t), \tag{4}$$

where $\boldsymbol{\sigma}(t)$, $\boldsymbol{\varepsilon}(t)$ and $\dot{\boldsymbol{\varepsilon}}(t)$ are the second-order stress, strain and strain rate tensors, respectively and $\boldsymbol{G}(t)$ is the fourth-order relaxation tensor. This standard solid model can in most cases be inverted into an equivalent integral creep form. The fourth-order creep tensor $\boldsymbol{J}$ relates the strain to the stress history. In the Laplace–Carson domain (see hereafter) this is reflected by $\hat{\boldsymbol{J}} = \hat{\boldsymbol{G}}^{-1}$. For an isotropic material, the relaxation tensor has the following expression:

$$\boldsymbol{G}(t) = 2G(t)\boldsymbol{I} + \left(K(t) - \frac{2}{3}G(t)\right)\boldsymbol{1}\otimes\boldsymbol{1}, \tag{5}$$

where $\boldsymbol{I}$ and $\boldsymbol{1}$ are the symmetric fourth- and second-order identity tensors, respectively, and $K(t)$ and $G(t)$ the bulk and shear moduli.

If $\boldsymbol{\varepsilon}(t)$ is a continuous and piece-wise differentiable function of time, the linear viscoelastic stress–strain relation (4) can be transformed by applying LCT (2) on both of its sides, leaving us after some simple manipulations with:

$$\hat{\boldsymbol{\sigma}}(s) = \hat{\boldsymbol{G}}(s) : \hat{\boldsymbol{\varepsilon}}(s), \quad \text{i.e. } \hat{\sigma}_{ij}(s) = \hat{G}_{ijnm}(s)\hat{\varepsilon}_{mn}(s). \tag{6}$$

Each component $\hat{G}_{ijkl}(s)$ of the fourth-order tensor $\hat{\boldsymbol{G}}(s)$ is the LCT of $G_{ijkl}(t)$. It is a complex function of the complex variable s. As already illustrated in Section 2.1, taking the $\hat{G}_{ijkl}(s)$ for $s = i\omega$ provides us with a means to completely characterize the frequency response of the material. Examples in connection with the numerical simulations of Section 6 are given hereafter. For isotropic materials, the complex tensile modulus is computed with help of the fourth-order creep tensor in the complex plane:

$$E^*(\omega) = \frac{1}{\hat{J}_{1111}(i\omega)}. \tag{7}$$

For transversely isotropic materials with anisotropy axis along the third direction, the complex transverse plane strain tensile modulus is given by

$$E^*_{12,2}(\omega) = \hat{G}_{1111}(i\omega) - \frac{\hat{G}_{1122}(i\omega)\hat{G}_{2211}(i\omega)}{\hat{G}_{2222}(i\omega)}. \tag{8}$$

3. Homogenization of multi-phase linear viscoelastic composites

Taking advantage of the correspondence principle, the prediction of the frequency behavior of heterogeneous viscoelastic solids is not more difficult than the prediction of the overall mechanical properties of multi-phase elastic composites. The problem is brought from time to complex domain where a two-step homogenization procedure is performed. In order to obtain storage and loss moduli characterizing the response of the material just a change of variable is needed as shown in Section 2.2.

3.1. Full analogy with linear elasticity

Let the representative volume element (RVE) Ω of a multi-phase composite be a matrix with N families of spheroidal inclusions. Each family Ω^i with volume fraction v^i inside the RVE is characterized by an aspect ratio A_{r_i} and a relaxation tensor $\boldsymbol{G}_i(t)$. Let also $\psi_i(\boldsymbol{p})$ be the orientation distribution function describing the orientation of the inclusions belonging to family i. The matrix Ω^0 has concentration v^0 and a relaxation tensor $\boldsymbol{G}_0(t)$. The term phase will be used to denote a family (phase i for $1 \leqslant i \leqslant N$) or the matrix (phase 0). Each phase's material is linear viscoelastic and homogeneous with a constitutive law given by (4).

Let the RVE be subjected to linear boundary displacement $\boldsymbol{u}(\boldsymbol{x},t)$ and apply the LCT (2) on the time variable t for all involved equations (i.e. constitutive equations, boundary conditions,...). What we get is a fictitious RVE in the Laplace–Carson domain (variable s) with boundary conditions $\hat{\boldsymbol{u}}(\boldsymbol{x},s)$ and for which the material behavior of each phase $1 \leqslant i \leqslant N$ is given by

$$\hat{\boldsymbol{\sigma}}(\boldsymbol{x},s) = \hat{\boldsymbol{G}}_i(s) : \hat{\boldsymbol{\varepsilon}}(\boldsymbol{x},s); \quad \forall \boldsymbol{x} \in \Omega^i. \tag{9}$$

This situation is identical to that of a multi-phase composite with homogeneous linear elastic reinforcements (see Camacho et al., 1990; Lielens, 1999; Pierard et al., 2004). Any homogenization procedure valid for these latter materials can thus be extended and applied to predict the frequency behavior of multi-phase viscoelastic composites.

3.2. A general two-step homogenization procedure

A general two-step homogenization procedure proposed in linear elasticity is applied here on the modified problem—the LCT of the original one—by keeping in mind that we are working with the complex variable s. The starting point of the method is the decomposition of the RVE into a set of pseudo-grains (see Fig. 1). Each pseudo-grain $\Omega_{i,\boldsymbol{p}}$ is a two-phase composite containing the matrix material and all the inclusions of family (i) aligned in direction $\boldsymbol{p}$. The relative volume fraction of the reinforcements in a pseudo-grain is set to $(1 - v^0)$. The idea is the following. As illustrated on Fig. 1, each pseudo-grain is first homogenized individually with a suitable scheme for this kind of composite. Afterwards the set of homogeneous pseudo-grains is itself homogenized. At the end, a volume average over the entire RVE is obtained as an average over families and orientations of the volume averages over the pseudo-grains:

$$\langle \bullet \rangle_\Omega = \sum_{i=1}^{N} \frac{v_i}{(1-v_0)} \oint \langle \bullet \rangle_{\Omega_{i,\boldsymbol{p}}} \mathrm{d}\psi_i(\boldsymbol{p}) \doteq \left\langle \langle \bullet \rangle_{\Omega_{i,\boldsymbol{p}}} \right\rangle_{i,\Psi_i}. \tag{10}$$

The derivation of the above formula is done as follows:

$$\langle \bullet \rangle_\Omega = \frac{1}{V(\Omega)} \sum_{i=1}^{N} V\left(\bigcup_{\boldsymbol{p}} \Omega_{i,\boldsymbol{p}} \right) \langle \bullet \rangle_{\bigcup_{\boldsymbol{p}} \Omega_{i,\boldsymbol{p}}} = \sum_{i=1}^{N} \oint \langle \bullet \rangle_{\Omega_{i,\boldsymbol{p}}} \frac{\mathrm{d}V(\Omega_{i,\boldsymbol{p}})}{V(\Omega)}, \tag{11}$$

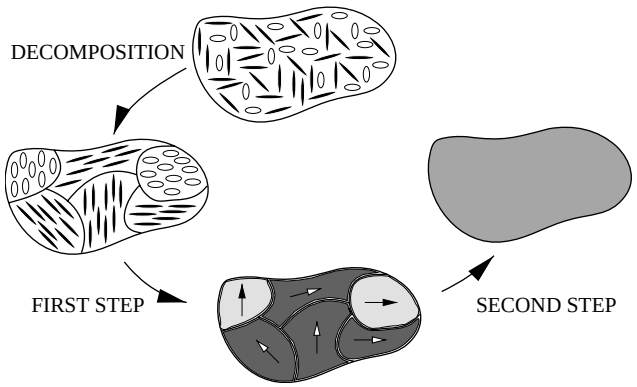

Fig. 1. The two-step homogenization procedure. The composite is decomposed into pseudo-grains. Step 1: homogenization of each pseudo-grain. Step 2: homogenization of the set of homogenized pseudo-grains.

with

$$\frac{\mathrm{d}V(\Omega_{i,\boldsymbol{p}})}{V(\Omega)} = \frac{v_i}{(1-v_0)}\,\mathrm{d}\psi_i(\boldsymbol{p}), \tag{12}$$

expressing the volume conservation of the inclusions of a given family aligned in a given direction inside the corresponding pseudo-grain and inside the entire RVE.

3.2.1. Homogenization of each pseudo-grain

Let $\Omega^1_{i,\boldsymbol{p}}$ and $\Omega^0_{i,\boldsymbol{p}}$, respectively be the inclusion and matrix phases of the pseudo-grain $\Omega_{i,\boldsymbol{p}}$ and $\hat{\boldsymbol{B}}^{\varepsilon}{}_{i,\boldsymbol{p}}(s)$ the related strain concentration tensor, i.e.

$$\langle\hat{\boldsymbol{\varepsilon}}(\boldsymbol{x},s)\rangle_{\Omega^1_{i,\boldsymbol{p}}} = \hat{\boldsymbol{B}}^{\varepsilon}{}_{i,\boldsymbol{p}}(s) :: \langle\hat{\boldsymbol{\varepsilon}}(\boldsymbol{x},s)\rangle_{\Omega^0_{i,\boldsymbol{p}}}. \tag{13}$$

Once defined, a strain concentration tensor gives rise to an effective relaxation tensor

$$\hat{\overline{\boldsymbol{G}}}_{i,\boldsymbol{p}}(s) = \left[(1-v_0)\hat{\boldsymbol{G}}_i(s) :: \hat{\boldsymbol{B}}^{\varepsilon}{}_{i,\boldsymbol{p}}(s) + v_0\hat{\boldsymbol{G}}_0(s)\right] : \left[(1-v_0)\hat{\boldsymbol{B}}^{\varepsilon}{}_{i,\boldsymbol{p}}(s) + v_0\boldsymbol{I}\right]^{-1} \tag{14}$$

that links average stress and strain at pseudo-grain level

$$\langle\hat{\boldsymbol{\sigma}}(\boldsymbol{x},s)\rangle_{\Omega_{i,\boldsymbol{p}}} = \hat{\overline{\boldsymbol{G}}}_{i,\boldsymbol{p}}(s) :: \langle\hat{\boldsymbol{\varepsilon}}(\boldsymbol{x},s)\rangle_{\Omega_{i,\boldsymbol{p}}}. \tag{15}$$

Simple homogenization schemes are obtained by assuming the same strain (Voigt) or stress (Reuss) in both phases of the pseudo-grain. These assumptions respectively lead to overestimate and underestimate the overall stiffness of this two-phase composite. In addition neither the shape of the inclusions nor their orientation are taken into account. More elaborated methods make up for these shortcomings and base their foundations on Eshelby's result (Eshelby, 1961). The latter is still valid here because the only difference with the linear elastic case is that every quantity depends now on the complex variable s.

The M–T model was proposed by Mori and Tanaka (1973) and takes into account, in an average way, the interactions between the inclusions. The strain concentration tensor for the M–T scheme is

$$\hat{\boldsymbol{B}}^{\varepsilon}{}_{i,\boldsymbol{p}}(s) = \left(\boldsymbol{I} + \boldsymbol{S}_{I,\hat{\boldsymbol{G}}_0(s)} : \left(\hat{\boldsymbol{G}}_0^{-1}(s) :: \hat{\boldsymbol{G}}_i(s) - \boldsymbol{I}\right)\right)^{-1} \doteq \boldsymbol{B}_{\mathrm{MT}}(s), \tag{16}$$

where $\boldsymbol{S}_{I,\hat{\boldsymbol{G}}_0(s)}$ is Eshelby's tensor with I corresponding to the inclusions with aspect ratio A_{r_i} aligned in direction $\boldsymbol{p}$. This expression is found to be identical to the one of the single inclusion problem (an inclusion

isolated inside an infinite matrix submited to a uniform remote strain field). Consequently, Benveniste (1987) proposed the following interpretation of the M–T model: each inclusion behaves like an isolated inclusion in the matrix seeing the average deformation in the matrix phase as a far-field strain. When the matrix is isotropic, $\boldsymbol{S}_{I,\hat{\boldsymbol{G}}_0(s)}$ is computed with help of the classical analytical formulae (see Eshelby, 1961; Mura, 1987) called with the LCT of the matrix material's Poisson's ratio $\hat{\nu}_0(s)$. There is no restriction upon the imaginary part of the Poisson's ratios.

The interpolative D–I model is based on the Nemat-Nasser and Hori (1999) double-inclusion model and was proposed by Lielens (1999). Inverting material properties between the matrix and the inclusion phases, we get the inverse M–T strain concentration tensor

$$\hat{\boldsymbol{B}}^{\varepsilon}{}_{i,\boldsymbol{p}}(s) = \boldsymbol{I} + \boldsymbol{S}_{I,\hat{\boldsymbol{G}}_i(s)} : \left(\hat{\boldsymbol{G}}_i^{-1}(s) : \ \hat{\boldsymbol{G}}_0(s) - \boldsymbol{I}\right) \doteq \boldsymbol{B}_{\mathrm{IMT}}(s). \tag{17}$$

Lielens (1999) proposed to interpolate between these two estimates to define a new concentration tensor as

$$\hat{\boldsymbol{B}}^{\varepsilon}{}_{i,\boldsymbol{p}}(s) = \left((1-f(v))\boldsymbol{B}_{\mathrm{MT}}^{-1}(s) + f(v)\boldsymbol{B}_{\mathrm{IMT}}^{-1}(s)\right)^{-1}, \tag{18}$$

with $f(v)$ a function of the volume fraction of inclusions. For the D–I model, the concentration of inclusions is explicitly part of the strain concentration tensor. Following the author the interpolation function is set to $f(v) = (v + v^2)/2$.

Both M–T and D–I models are used in our numerical simulations in Section 6.

3.2.2. Homogenization of the set of homogenized pseudo-grain

To perform the second step we will assume that each homogenized pseudo-grain undergoes the same deformation. The macroscopic relaxation tensor that links average stress and strain over the RVE is then given by

$$\overline{\hat{\boldsymbol{G}}}(s) = \left\langle \overline{\hat{\boldsymbol{G}}}_{i,\boldsymbol{p}}(s) \right\rangle_{i,\Psi_i}. \tag{19}$$

Using this Voigt-like hypothesis leads in general to better results compared to those obtained by assuming that the pseudo-grains are sharing the same stress or by using M–T (same deformation in the matrix phase of all pseudo-grains) to perform the step. In linear elasticity (see e.g. Camacho et al., 1990; Pierard et al., 2004) as well as for elasto-plastic composites (see e.g. Doghri and Tinel, 2005), very good predictions are obtained in many situations. Indeed the Voigt-like assumption can be intuitively understood (see Christensen, 1992; Lielens, 1999) by thinking of a two-phase composite with misaligned long fibers. The RVE for this composite may consist of mingled fibers crossing the boundaries. For the average strain in each fiber to be compatible with the average strain imposed on the RVE, the displacement of each fiber must follow the displacement of the surface it crosses. The fibers are thus acting in parallel. To achieve that in the two-step model, we must suppose the same deformation in all pseudo-grains. The Voigt-like assumption seems therefore to be more appealing than the others. The M–T assumption should even be rejected because it might lead to physically unacceptable results (see Benveniste et al., 1991; Pierard et al., 2004). The case of a three-phase composite involving two sets of aspect ratios constitutes a classical example.

4. Three general approaches for composites with coated inclusions

In Section 1, we discussed several methods for coated inclusion-reinforced materials. In this section, we focus on general approaches and propose two new ones: two-level and two-step schemes. The composites studied here are made up of three phases: matrix, inclusions and coaxial coatings. All inclusions have the same aspect ratio and orientation. There are three linear elastic materials, one for each phase. It is also

assumed that both reinforcing phases have the same shape (identical aspect ratios). This correponds to most-frequently encountered situations (e.g., spherical particles or long fibers coated with constant thickness layers).

All the restrictions above are introduced for clarity only as none of them is really a limitation. Firstly, as underlined in the previous sections, the correspondence principle enables to transfer results from elasticity to viscoelasticity. Secondly, dealing with much more general multi-phase composites with coated inclusions, the virtual decomposition step of the two-step homogenization procedure (Fig. 1) leads to three-phase pseudo-grains of the type studied here. The following methods should then be used to achieve the first step (homogenization of each pseudo-grain), the second step remaining unchanged.

4.1. A two-level recursive scheme

We propose a two-level procedure based on the idea that the matrix sees reinforcements that are themselves composites. We thus propose a two-level recursive application of homogenization schemes. As illustrated on Fig. 2, each coated inclusion is seen (deepest level) as a two-phase composite (a single inclusion inside a matrix made of the interphase material) which, once homogenized, plays the role of a homogeneous reinforcement for the matrix material (highest level). At each level a homogenization scheme suitable for two-phase materials is needed. Using Eshelby-based methods supposes that the effective properties at the deepest level are the same as those of a matrix body made of interphase material and reinforced with a large number of small and randomly positioned inclusions having the same aspect ratio and volume fraction as the real ones.

Several remarks must be made about this recursive scheme. Suppose that each material is isotropic. At the highest level we have to deal with homogeneous transversely isotropic inclusions—the outcome of the deepest level. One must then care about the calculation of Eshelby's tensor when using Lielens interpolative model (Lielens, 1999): the transversely isotropic material will also play the role of the matrix. Nevertheless, Eshelby's result is still valid and analytical formulae (see Withers, 1989) still exist provided the revolution axis of the spheroid is aligned with the matrix' principal direction—which is the case here. At the deepest

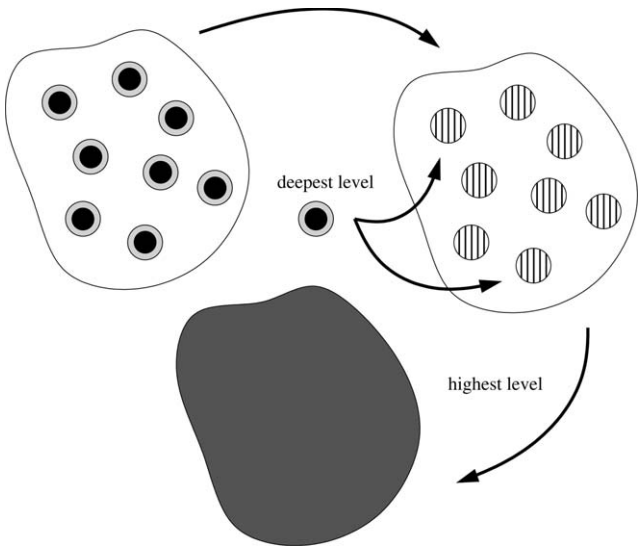

Fig. 2. The two-level recursive homogenization procedure. The coated inclusions are seen as two-phase composites. Once homogenized (deepest level) they play the role of reinforcements to complete the homogenization (highest level).

level both materials are isotropic but the volume fraction of fillers is in general high. The interpolative D–I scheme or even the inverse M–T model may thus be more adapted for this level than the M–T model.

4.2. Other procedures

Another generic way to handle coatings is through the multi-inclusion method by Nemat-Nasser and Hori (1999) which is an extension of their double-inclusion model. For a three-phase composite with coatings the behavior is approximated by that of an inclusion coated with a layer of interphase, itself surrounded by a layer of matrix and embedded inside a reference material (Fig. 3(a)). Nemat-Nasser and Hori (1999) showed that the overall stiffness tensor obtained with this multi-inclusion method is identical to the one predicted by their multi-phase composite model. In other words, the coatings behave as if they were a separate phase in matrix: inside the reference material stays an inclusion of matrix embedding separate inclusions of the other components (Fig. 3(b)). To make things simple, choosing as reference material the one of the matrix will lead in both cases to the well known generalized M–T scheme where the coatings are considered as a distinct reinforcing phase (Fig. 4(b)).

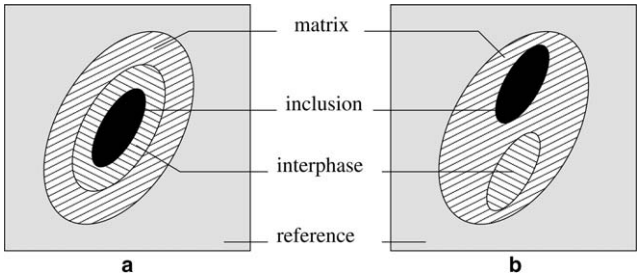

Fig. 3. Schematic view of the multi-inclusion method (a) and the multi-phase composite model (b) by Nemat-Nasser and Hori (1999).

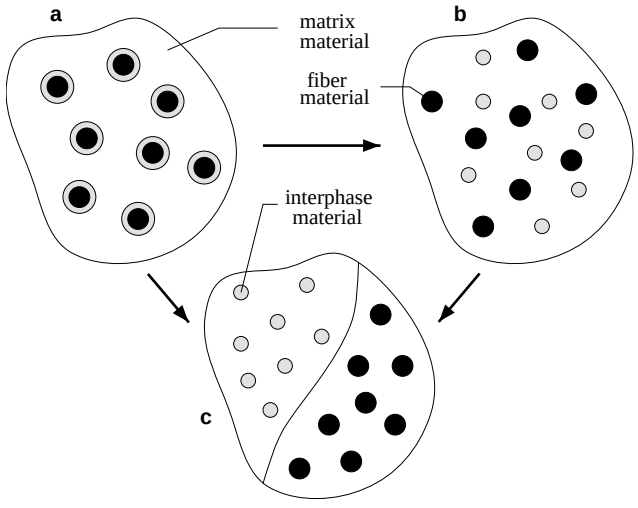

Fig. 4. (a) Transverse view of a coated fiber composite. (b) Direct extension of the Mori–Tanaka model: a three-phase composite without interphase. (c) The two-step procedure: pseudo-grains of two types, (matrix + real inclusions) and (matrix + inclusions made of interphase material).

4.3. A two-step method

We propose a two-step scheme which treats coatings as separate reinforcements but instead of using a generalized M–T for the three-phase coated composite, we virtually decompose the composite into an aggregate of two pseudo-grains, each containing the matrix material either reinforced with real inclusions or with inclusions made of coating material (Fig. 4(c)). Each two-phase pseudo grain is homogenized (first step) and then the effective properties of the aggregate are computed (second step). We suggest using interpolative D–I or M–T in the first step and Voigt in the second.

Examples in Section 6 show that under severe conditions, our proposed two-level and two-step schemes give remarkable predictions while a direct M–T method leads to erroneous results.

4.4. A comparative study

In order to exhibit the differences between those three procedures, the effective stiffness tensors are hereafter developed for generalized M–T, the two-step (M–T, Voigt) and the two-level (M–T, M–T) schemes. The three phases are denoted Ω^0 (matrix), Ω^1 (real inclusions) and Ω^2 (real coatings) while Ω stands for the composite. Volume fractions of components inside the composite are denoted v_i and elastic tensors $\boldsymbol{C}_i$ for $i = 0, 1, 2$. We also introduce the following notation:

$$\boldsymbol{B}^{\varepsilon}_{\boldsymbol{C}_i,\boldsymbol{C}_j} = \left(\boldsymbol{I} + \boldsymbol{S}_{I,\boldsymbol{C}_i} : \left(\boldsymbol{C}_i^{-1} : \boldsymbol{C}_j - \boldsymbol{I}\right)\right)^{-1}. \tag{20}$$

For a matrix material $\boldsymbol{C}_i$ reinforced with aligned inclusions of material $\boldsymbol{C}_j$ and shape I, this is the expression of the strain concentration tensor relating strain averages between inclusion and matrix phases that corresponds to the M–T scheme.

- The direct extension of the M–T scheme handles the coated inclusions as if they were not coated (Fig. 4(b)). The overall stiffness tensor reads

$$\overline{\boldsymbol{C}} = \boldsymbol{C}_0 + v_1(\boldsymbol{C}_1 - \boldsymbol{C}_0) : \boldsymbol{A}^{\varepsilon}_1 + v_2(\boldsymbol{C}_2 - \boldsymbol{C}_0) : \boldsymbol{A}^{\varepsilon}_2, \tag{21}$$

where $\boldsymbol{A}^{\varepsilon}_1$ and $\boldsymbol{A}^{\varepsilon}_2$ are the strain concentration tensors linking average strains in each reinforcing phase to the average strains in the composite:

$$\langle\boldsymbol{\varepsilon}\rangle_{\Omega^i} = \boldsymbol{A}^{\varepsilon}_i : \langle\boldsymbol{\varepsilon}\rangle_{\Omega}; \quad \boldsymbol{A}^{\varepsilon}_i = \boldsymbol{B}^{\varepsilon}_{\boldsymbol{C}_0,\boldsymbol{C}_i} : \left(v_0\boldsymbol{I} + v_1\boldsymbol{B}^{\varepsilon}_{\boldsymbol{C}_0,\boldsymbol{C}_1} + v_2\boldsymbol{B}^{\varepsilon}_{\boldsymbol{C}_0,\boldsymbol{C}_2}\right)^{-1}; \quad i = 1, 2. \tag{22}$$

- The two-step (M–T, Voigt) model leads to the definition of two pseudo-grains (Fig. 4(c)) Ω_{01} (matrix + real inclusions) and Ω_{02} (matrix + inclusions made of interphase material). The macroscopic stiffness

$$\overline{\boldsymbol{C}} = \boldsymbol{C}_0 + v_1(\boldsymbol{C}_1 - \boldsymbol{C}_0) : \ \boldsymbol{A}^{\varepsilon}_{1,01} + v_2(\boldsymbol{C}_2 - \boldsymbol{C}_0) : \ \boldsymbol{A}^{\varepsilon}_{2,02} \tag{23}$$

has a similar expression (compare (23) to (21)) except that the concentration tensors do not relate the same quantities as before. Each makes the link between average strains in the inclusion phase of a pseudo-grain (Ω^1_{01} or Ω^1_{02}) and the macro strains in that pseudo-grain:

$$\langle\boldsymbol{\varepsilon}\rangle_{\Omega^1_{0i}} = \boldsymbol{A}^{\varepsilon}_{i,0i} : \langle\boldsymbol{\varepsilon}\rangle_{\Omega_{0i}}; \quad \boldsymbol{A}^{\varepsilon}_{i,0i} = \boldsymbol{B}^{\varepsilon}_{\boldsymbol{C}_0,\boldsymbol{C}_i} : \left(v_0\boldsymbol{I} + (1 - v_0)\boldsymbol{B}^{\varepsilon}_{\boldsymbol{C}_0,\boldsymbol{C}_i}\right)^{-1}; \quad i = 1, 2. \tag{24}$$

- In the two-level (M–T, M–T) scheme, we first homogenize the coated inclusions with M–T. We thus obtain an effective stiffness

$$\overline{\boldsymbol{C}}_{21} = \boldsymbol{C}_2 + \frac{v_1}{v_1 + v_2}(\boldsymbol{C}_1 - \boldsymbol{C}_2) : \boldsymbol{A}^{\varepsilon}_{1,21}, \tag{25}$$

where the concentration tensor $\boldsymbol{A}^{\varepsilon}_{1,21}$ considers the inclusions as the reinforcing phase Ω^1_{21} of the aggregate Ω_{21} (inclusions + coatings) and relates the average strains as follows:

$$\langle\boldsymbol{\varepsilon}\rangle_{\Omega^1_{21}} = \boldsymbol{A}^{\varepsilon}_{1,21} : \langle\boldsymbol{\varepsilon}\rangle_{\Omega_{21}}; \quad \boldsymbol{A}^{\varepsilon}_{1,21} = (v_1+v_2)\boldsymbol{B}^{\varepsilon}_{\boldsymbol{C}_2,\boldsymbol{C}_1} : \left(v_2\boldsymbol{I} + v_1\boldsymbol{B}^{\varepsilon}_{\boldsymbol{C}_2,\boldsymbol{C}_1}\right)^{-1}. \tag{26}$$

Next, we homogenize the matrix reinforced with those homogenized inclusions. As expected, this leads to an expression which is nested with the (25):

$$\overline{\boldsymbol{C}} = \boldsymbol{C}_0 + (v_1+v_2)(\overline{\boldsymbol{C}}_{21} - \boldsymbol{C}_0) : \boldsymbol{A}^{\varepsilon}_{21}. \tag{27}$$

Moreover, the strain concentration tensor $\boldsymbol{A}^{\varepsilon}_{21}$ depends also on the deepest level overall stiffness $\overline{\boldsymbol{C}}_{21}$ and reads for the M–T scheme:

$$\langle\boldsymbol{\varepsilon}\rangle_{\Omega_{21}} = \boldsymbol{A}^{\varepsilon}_{21} : \langle\boldsymbol{\varepsilon}\rangle_{\Omega}; \quad \boldsymbol{A}^{\varepsilon}_{21} = \boldsymbol{B}^{\varepsilon}_{\boldsymbol{C}_0,\overline{\boldsymbol{C}}_{21}} : \left(v_0\boldsymbol{I} + (v_1+v_2)\boldsymbol{B}^{\varepsilon}_{\boldsymbol{C}_0,\overline{\boldsymbol{C}}_{21}}\right)^{-1}. \tag{28}$$

For the differences to be better underlined, the average strains in the coated phase (i.e., the real inclusions) are written with respect to the macro strains $\langle\boldsymbol{\varepsilon}\rangle_{\Omega}$ for each one of the three methods:

$$\langle\boldsymbol{\varepsilon}\rangle_{\Omega^1} = \boldsymbol{A}^{\varepsilon}_1 : \langle\boldsymbol{\varepsilon}\rangle_{\Omega}, \tag{29}$$

$$\langle\boldsymbol{\varepsilon}\rangle_{\Omega^1} = \boldsymbol{A}^{\varepsilon}_{1,01} : \langle\boldsymbol{\varepsilon}\rangle_{\Omega}, \tag{30}$$

$$\langle\boldsymbol{\varepsilon}\rangle_{\Omega^1} = \boldsymbol{A}^{\varepsilon}_{1,21} : \boldsymbol{A}^{\varepsilon}_{21} : \langle\boldsymbol{\varepsilon}\rangle_{\Omega}. \tag{31}$$

In the two-step scheme (Eq. (30)) the average deformation in the real inclusions does not depend on what happens in the coatings, because of the Voigt assumption in the second step (under appplied strain). For the direct extension of the M–T model (Eq. (29)) the deformations in the coated and the coating phases are linked ($\boldsymbol{A}^{\varepsilon}_1$ also involves $\boldsymbol{B}^{\varepsilon}_{\boldsymbol{C}_0,\boldsymbol{C}_2}$). This is also true for the two-level approach (Eq. (31)). This latter scheme exhibits a multiplicative decomposition of the strain concentration tensor. Note that a similar decomposition was found by Aboutajeddine and Neale (2005) in their new formulation of the double-inclusion model.

5. Time effective properties of multi-phase viscoelastic composites

Homogenization of viscoelastic multi-phase composites is not achieved in time domain. The LCT brings the whole problem into the complex domain. Taking advantage of similarities with elastic composites, homogenization schemes are extended in a straightforward manner, except that everything depends on the complex variable s. The frequency behavior comes out by a simple change of variable $s = \mathrm{i}\omega$. The overall time properties (e.g. how do the effective moduli evolve w.r.t. time?) cannot be obtained in such an easy way. A numerical inversion of the LCT is required. The collocation method proposed by Schapery (1962) is hereafter presented. It is easy to implement and the approximate function can be evaluated at any time once some coefficients are determined. The method was advocated by Masson (1998) and also successfully tested by Pierard and Doghri (2004) in the framework of the affine formulation for elasto-viscoplastic composites.

5.1. Principle of the collocation method

Let us consider an unknown time function $f(t)$ which we are able to evaluate at any point of the transformed domain, i.e. $\hat{f}(s)$ is known. The approximation $\tilde{f}(t)$ is developed into a n-terms Dirichlet series with an additional affine term,

$$\tilde{f}(t) = A + Bt + \sum_{k=1}^{k=n} b_k \underbrace{(1 - \mathrm{e}^{-t/\theta_k})}_{\text{basis functions}}, \tag{32}$$

and its transform is fitted with the transform of the series over a number m of distinct points, i.e.

$$\hat{f}(s_l) = A + \frac{B}{s_l} + \sum_{k=1}^{k=n} \frac{b_k}{1 + s_l\theta_k}, \quad 1 \leqslant l \leqslant m. \tag{33}$$

The above relations constitute a linear system with $n + 2$ unknowns: A, B and b_k for $1 \leqslant k \leqslant n$. The number of variables is reduced to n since

$$A = \lim_{s\to+\infty} \hat{f}(s) = \lim_{t\to 0} f(t), \tag{34}$$

$$B = \lim_{s\to 0} s\hat{f}(s) = \lim_{t\to+\infty} \frac{f(t)}{t}, \tag{35}$$

giving the sufficient condition $m \geqslant n$ to ensure uniqueness of the solution of the system (33) in a least square sense. Once the unknowns fixed, the function f can be estimated at any time t with help of (32). Following Schapery (1962) the total square error between the function and its approximation $(\int_0^\infty (f(t) - \tilde{f}(t))^2 \,\mathrm{d}t)$ is minimized by collocating the LCT of the Dirichlet series and $\hat{f}$ at n points $s = 1/\theta$ (i.e. $m = n$ and $s_k = 1/\theta_k$; $1 \leqslant k \leqslant n$).

5.2. Application to viscoelastic composites

The unknown time function is in this case a tensor: the effective fourth-order relaxation tensor $\overline{\boldsymbol{G}}$. As each component G_{ijkl} is only a function of time, the generalization of the aforementioned procedure is obvious.

The shape of the basis functions is similar to the terms of a Prony series (see (36)). The set of collocation points θ_k should then at least contain all the relaxation times of all the materials involved in the composite. This is however not enough and most authors advise to choose about twenty equispaced points on a logarithmic scale (see e.g. Pierard and Doghri, 2004).

The last issue is the limit tensors, $\boldsymbol{A}$ and $\boldsymbol{B}$, which have to be known whatever the homogenization procedure. This is actually not a problem: $\boldsymbol{A}$ corresponds to the initial elastic response and $\boldsymbol{B}$ vanishes since $\overline{\boldsymbol{G}}(t)$ remains finite for each t.

6. Numerical simulations

All the theorical aspects exposed up to here, namely the two-step homogenization procedure (Section 3), the two-level and two-step approaches for coatings (Section 4) and the collocation method (Section 5) are hereafter applied to predict the frequency and time behavior of viscoelastic composites with two or three phases, including coatings. Nineteen distinct composites are presented: fifteen two-phase materials and four with three phases. Shear or (plane strain) tensile complex moduli are estimated with respect to frequency (5 cases), time (10 cases) or volume fraction of fillers (4 cases) using many different homogenization schemes. The latter are analyzed as often as possible and compared with respect to each other. Each time, the predictions are validated against experimental data and/or FE results taken from the literature.

6.1. Frequency behavior of two-phase viscoelastic composites

The numerical materials involved here are made of two phases for which at least one is viscoelastic. In all cases the inclusions are assumed aligned, reducing the two-step procedure to classical homogenization methods. M–T and Lielens' interpolative schemes are used to predict the shear or tensile complex modulus,

Table 1
Components' weight and volume fractions of the Paraloid particle reinforced (PVC + DOP) matrix composite studied by Redaelli (2002)

Materials	Matrix			Inclusions
	PVC	DOP	Stabilizers	Paraloid
Weight fraction [%]	61.5	24.5	1	13
Relative density[a] (water = 1) [−]	0.9	0.9861		0.9
Volume fraction [%]		86.71		13.29

[a] *Sources*: http://www.inchem.org, http://www.chemicalland21.com.

either with respect to frequency or, for a given one, in function of the volume fraction of fillers. The latter are spherical particles or long fibers. FE unit cell results and experimental data are used for validation.

6.1.1. PVC matrix with spherical Paraloid inclusions

The composite was prepared by Redaelli (2002). It involves two incompatible polymers, Paraloid—commercial name for polybutyl acrylate/methyl methacrylate—and polyvinyl chloride (PVC). The PVC had to be plasticized by adding dioctyl phtalate (DOP) and small quantities of stabilizers entered also in the preparation. The original composition was given in weight fractions of components. With help of the densities we computed the volume fraction of each phase (the 1% stabilizers were shared half and half between PVC and DOP). All these data are summarized in Table 1. Storage and loss shear moduli were determined experimentally by Redaelli (2002) for the matrix, the inclusions and the blend over a frequency range from 0.5 to 50 Hz. With regard to the geometry of the reinforcements, scanning electron analysis (SEM) images also coming from Redaelli (2002) show the Paraloid inclusions to be of spherical shape (i.e. $A_r = 1$).

The experimental measurements provided only the complex shear moduli. We calculated the bulk modulus of each phase with help of the Poisson's ratios which we assumed constant. The matrix (PVC + DOP) Poisson's ratio was fixed to 0.49 according to Chazeau et al. (1999) who studied DOP plasticized PVC—in proportions similar to the material of Redaelli (2002)—and reported a value of 0.5 at 280 K. The knowledge of the Paraloid Poisson's ratio is less important since it has no effect—at least for the M–T scheme—on the effective shear modulus. The value of 0.4 was used.

We made numerical simulations with the M–T model. Our estimates of the complex shear modulus are confronted to the experimental results on Figs. 5 and 6. The loss modulus is pretty well predicted (Fig. 6) while the storage one is sligthly overestimated (Fig. 5). One reason might be that the material used for the inclusion phase in our model is not pure Paraloid (no experimental data were reported in Redaelli (2002) for pure Paraloid at 0 °C) but plasticized Paraloid (Paraloid + DOP).

6.1.2. Epoxy and copolymer matrix materials reinforced with ceramic particles

Marra et al. (1999) studied two composites. Both consist of a polymeric matrix reinforced with Ca-modified $PbTiO_3$—a ceramic—spherical inclusions. The materials used for the matrix phase are Epon 828 and P(VDF-TrFE). For each of them, the authors made experimental measurements of the tensile storage and loss moduli. Next, they assumed constant (and thus real) Poisson's ratios—values were taken from the literature (see Marra et al., 1999) and references therein)—to compute the real and imaginary parts of the complex shear and bulk moduli. The reinforcing material is supposed elastic and its parameters were obtained from previous works of other authors (see Marra et al., 1999). The (visco)elastic parameters of these three components are reported in Table 2 for the angular frequency of interest $\omega = 10$ rad s^{-1}. Marra et al., 1999 collected experimental data on the complex tensile modulus for the heterogeneous materials. In addition, they made axisymmetric unit cell FE calculations and used a simple analytical model in order to predict the frequency behavior in tension. We made numerical simulations on these composites with the M–T

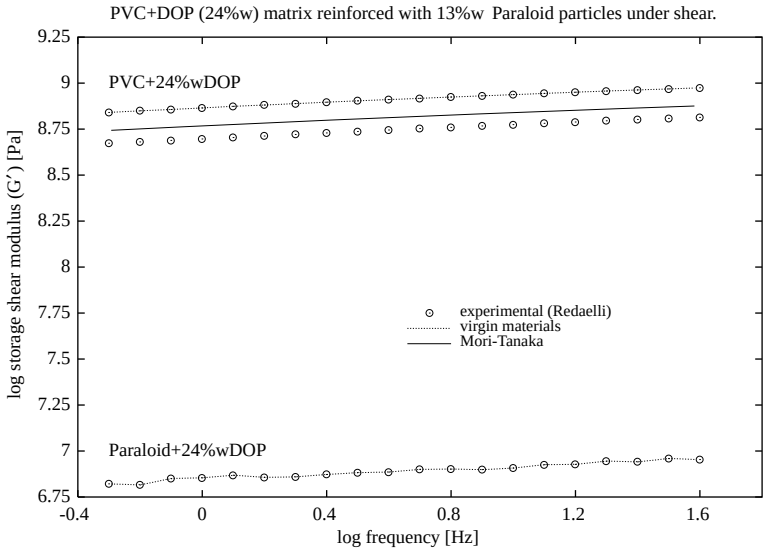

Fig. 5. Storage shear modulus as a function of frequency of a two-phase viscoelastic composite at 0 °C. Comparison between experimental measurements and estimates obtained with the Mori–Tanaka scheme.

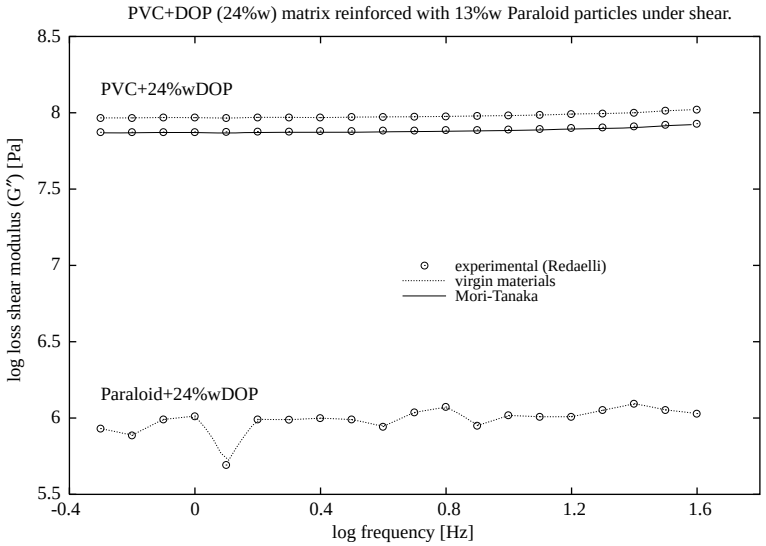

Fig. 6. Loss shear modulus as a function of frequency of a two-phase viscoelastic composite at 0 °C. Comparison between experimental measurements and estimates obtained with the Mori–Tanaka scheme.

scheme and the interpolative D–I model (D–I). The predictions we obtained are confronted to Marra et al. (1999) results on Figs. 7–10.

Looking at these four figures all together, one can observe that none of the numerical methods gives results very close to the experimental data. The misfit is much more pronounced for the tensile loss modulus than for the storage one (compare Figs. 8 and 10 to Figs. 7 and 9, resp.). The worst predictions are obtained

Table 2
Mechanical properties of Ca-modified $PbTiO_3$, Epon 828 and P(VDF-TrFE) for $\omega = 10$ rad s^{-1} (after Marra et al., 1999)

	G' [GPa]	G'' [GPa]	K' [GPa]	K'' [GPa]
Epon 828	1.2851	1.2524×10^{-2}	4.1560	4.0501×10^{-2}
P(VDF-TrFE)	5.6789×10^{-1}	2.0221×10^{-2}	2.4386	8.6832×10^{-2}
		E [GPa]		v [−]
Epon 828				0.36
P(VDF-TrFE)				0.392
Ca-modified $PbTiO_3$		127.6		0.2046

for the Ca-modified $PbTi0_3$/Epon 828 composite (Fig. 8). One reason for this bad behavior is that all these numerical simulations have been conducted with input data computed by assuming constant Poisson's ratios (see above). A real Poisson's ratio implies indeed the same time dependency for the shear, bulk and tensile moduli (e.g. identical relaxation times and normalized weights in the Prony series). The impact of such a restriction might be not negligible and may not be suitable for these materials, especially for Epon 828.

Comparing the three analytical models together with the experimental data, the M–T scheme does in most cases the worst job. That can be easily understood given the high volume fraction of fillers we must deal with. The interpolative model tackles this issue and provides predictions as close as (Figs. 7 and 9) or even closer to the experimental results (Figs. 8 and 10) than those obtained with the analytical model used by Marra et al. (1999). The latter model is based on Hashin (1962, 1970) and Christensen (1969) works. Exploiting the correspondence principle, it uses formulae for the bulk and shear elastic moduli of particle reinforced two-phase composites. As no further details were given in Marra et al. (1999) on which formulae they exactly used, we preferred reporting the corresponding curves as they were plotted. Nevertheless, we can say that apart from the geometrical restriction this model has some limitations: the inclusions are elastic, the matrix is viscoelastic in shear and elastic in hydrostatic loading, the square of the matrix shear loss factor is small (see Marra

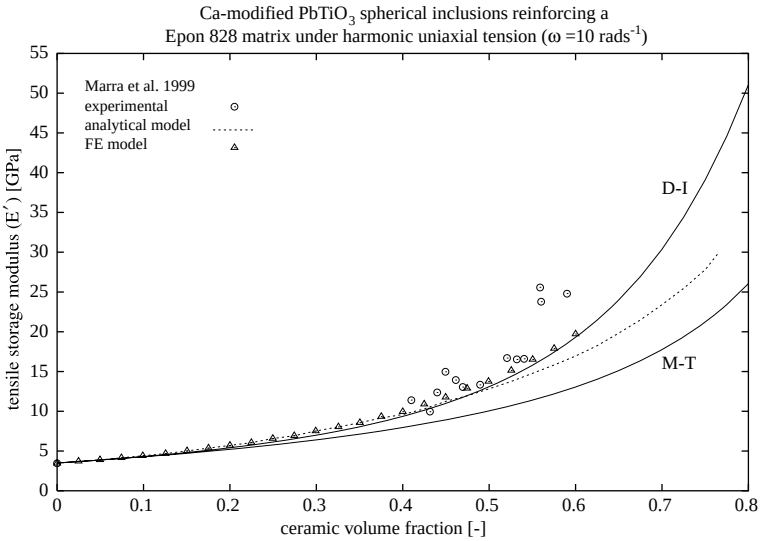

Fig. 7. Storage tensile modulus versus volume fraction of inclusions of a ceramic elastic particle reinforced Epon 828 viscoelastic matrix. Comparison between experimental results, FE calculations and various homogenization scheme predictions.

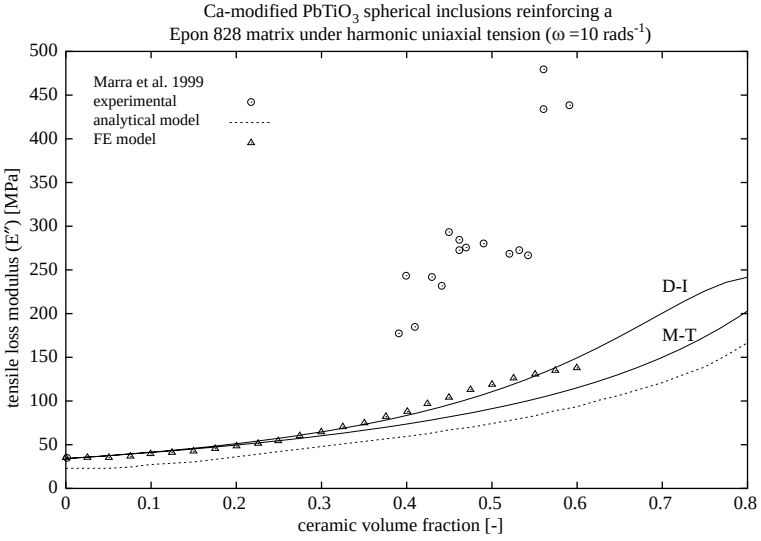

Fig. 8. Loss tensile modulus versus volume fraction of inclusions of a ceramic elastic particle reinforced Epon 828 viscoelastic matrix. Comparison between experimental results, FE calculations and various homogenization scheme predictions.

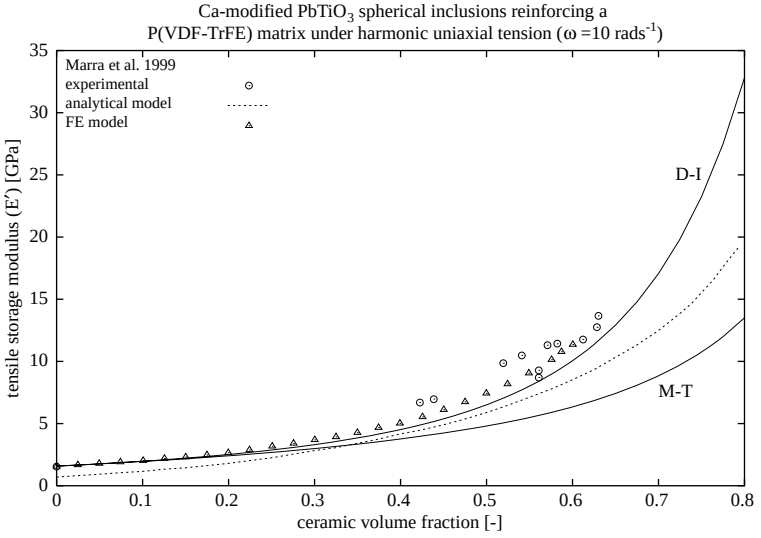

Fig. 9. Storage tensile modulus versus volume fraction of inclusions of a ceramic elastic particle reinforced P(VDF-TrFE) viscoelastic matrix. Comparison between experimental results, FE calculations and various homogenization scheme predictions.

et al., 1999). The interpolative scheme (D–I) does not suffer from any of these shortcomings and we could even hope better predictions if we knew the shear behavior of the two polymers. Moreover, the agreement between the D–I predictions and the FE results is always very satisfying (see Figs. 7–10). However, the FE analyses require for every volume fraction of reinforcements a different FE mesh, and this is very consuming in user time. As far as CPU time in concerned, a D–I simulation for a particle concentration ranging from 0 to 1 lasts less than a second on an ordinary PC (CPU: 333 MHz, RAM: 160 M).

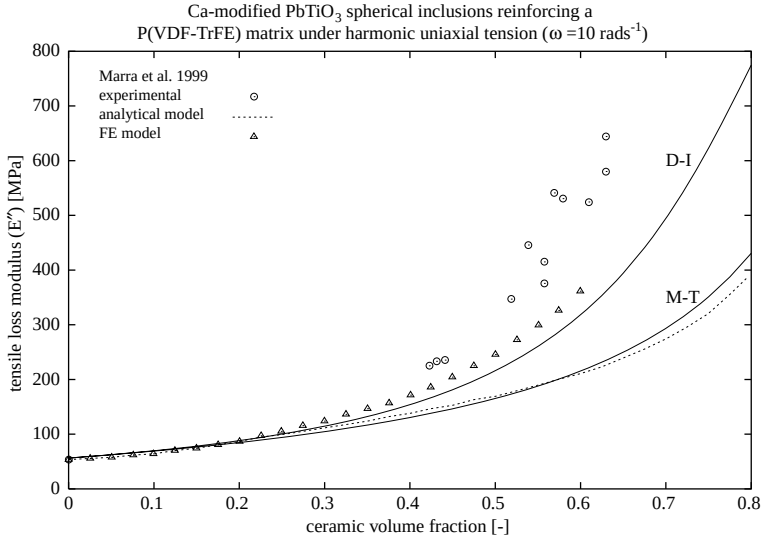

Fig. 10. Loss tensile modulus versus volume fraction of inclusions of a ceramic elastic particle reinforced P(VDF-TrFE) viscoelastic matrix. Comparison between experimental results, FE calculations and various homogenization scheme predictions.

6.1.3. Viscoelastic matrix with long viscoelastic fibers

The components involved in the composite explored by Brinson and Lin (1998) are two idealized isotropic viscoelastic materials. Prony series are used to describe the time evolution of their shear and bulk moduli:

$$Y(t) = Y_0\left[1 - \sum_{i=1}^{n} w_i\left(1 - \mathrm{e}^{-t/\tau_i}\right)\right], \quad Y_0 = Y(t=0). \tag{36}$$

The relaxation times (τ_i) and weights ($w_i Y_0$) are listed on Table 3 for both materials' moduli. The sets of values were chosen so that one of the materials is at all times stiffer (the stiff material) than the other (the soft material) and that their loss peaks do not coincide. Notice also that in both cases shear and bulk moduli do not have the same time dependence. The complex Poisson's ratios have therefore a non-zero imaginary part. Both materials will alternatively play the role of the matrix and the inclusions with a volume fraction of stiff material always equal to 36%.

This time the reinforcements are no longer of spherical shape but consist of long fibers ($A_r \to \infty$), resulting in transversely isotropic heterogeneous materials. Brinson and Lin (1998) were interested in the complex transverse plane strain tensile modulus of these two composites. To this end, they made FE calculations with two sorts of unit cells. The models differed by the fiber arrangement in the matrix: square (FE-SQR) and hexagonal (FE-HEX) array (see Brinson and Lin, 1998, for details). The authors also made simulations with the M–T scheme.

We compare our interpolative D–I and M–T predictions of the composites' storage and loss moduli to those FE results on Figs. 11 and 12. In all cases, the FE and the homogenization models predict similar frequency behaviors. However, the estimates obtained with the interpolative D–I match always the FE-HEX ones. This is very satisfying because the hexagonal array fiber arrangement is more likely to reflect the transverse isotropy of the material (Jansson, 1992). The M–T predictions—identical to those obtained by Brinson and Lin (1998)—are less satisfying for a fiber volume fraction of 64%. As in the linear elastic case (see Pierard et al., 2004) the analytical prediction is improved with the D–I model.

Table 3
Mechanical properties of the idealized viscoelastic materials used by Brinson and Lin (1998) and Fisher and Brinson (2001)

Stiff material				Soft material			
Shear		Bulk		Shear		Bulk	
τ_i [s]	$G_0 w_i$ [bar]	τ_i [s]	$K_0 w_i$ [bar]	τ_i [s]	$G_0 w_i$ [bar]	τ_i [s]	$K_0 w_i$ [bar]
3	3.162	10,000	40,000	0.032	2.512	100.000	3000
10	17.783			0.100	10.000	316.228	100
32	100.000			0.316	56.234		
100	316.228			1.000	316.228		
316	1000.000			3.162	1000.000		
1000	5623.413			10.000	199.526		
3162	10,000.000			31.623	50.119		
10,000	562.341			100.000	19.953		
31,623	141.254			316.228	12.589		
100,000	56.234			1000.000	2.512		
316,228	17.783			3162.278	1.698		
1,000,000	5.623			10,000.000	1.202		
3,162,278	3.162			31,622.777	1.148		
10,000,000	1.778			100,000.000	1.096		
$G_0 = 17{,}948.761$		$K_0 = 48{,}000$		$G_0 = 1677.979$		$K_0 = 3300$	

Relaxation times and weights involved in the Prony series.

6.2. Frequency behavior of coated-inclusion reinforced materials

The following composites are made of elastic fibers or particles coated with a viscoelastic material and embedded in a viscoelastic matrix. Various homogenization methods able to handle coatings are compared together: the two-step procedure, our original two-level method, the direct extension of the M–T scheme—

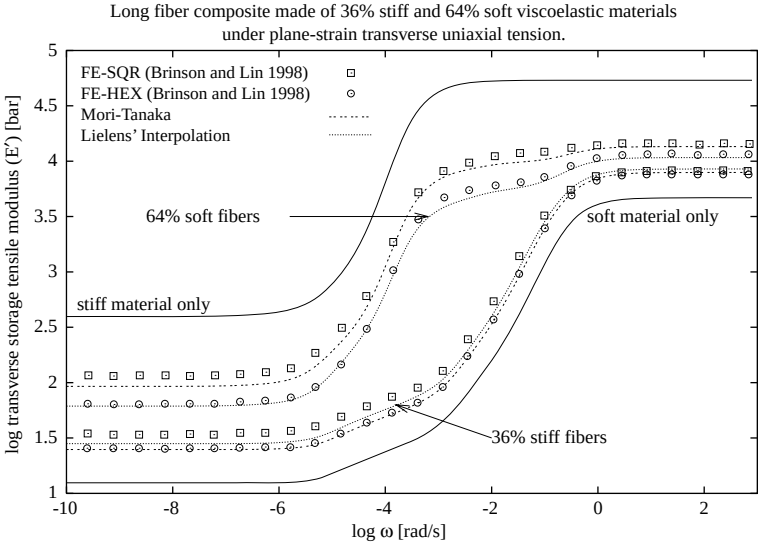

Fig. 11. Plane strain transverse storage tensile modulus as a function of frequency of two long fiber composites. Both phases bulk and shear moduli are described with Prony series. The interpolative and Mori–Tanaka schemes are confronted to two FE unit cells calculations.

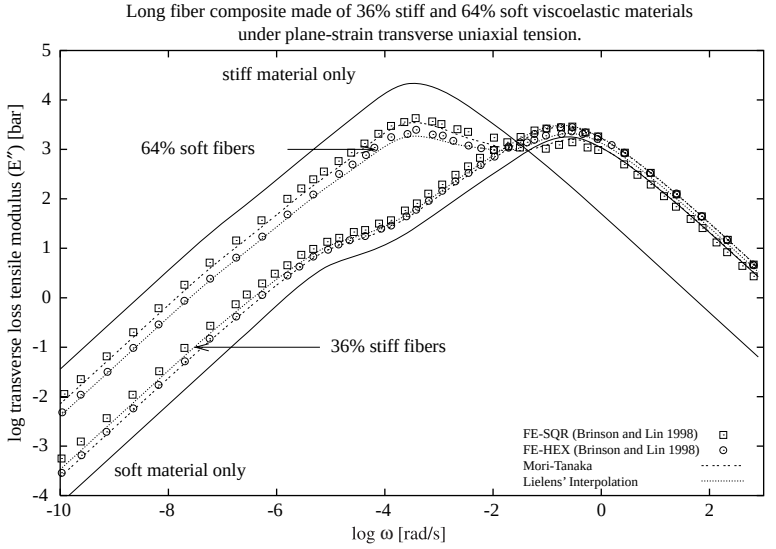

Fig. 12. Plane strain transverse loss tensile modulus as a function of frequency of two long fiber composites. Both phases bulk and shear moduli are described with Prony series. The interpolative and Mori–Tanaka schemes are confronted to two FE unit cells calculations.

which is a particular case of the Multi-Inclusion method of Nemat-Nasser and Hori—and Benveniste's model. The predicted complex tensile moduli (with respect to frequency or volume fraction of inclusions) are confronted to experimental data and/or FE calculations.

6.2.1. Viscoelastic matrix with long elastic fibers and viscoelastic coatings

Keeping both idealized viscoelastic materials of Table 3 and taking as third component an elastic one, Fisher and Brinson (2001) considered the following three-phase composites: 30% elastic long fibers reinforcing a soft (resp. stiff) viscoelastic matrix with 10% stiff (resp. soft) viscoelastic interphase. The fibers with elastic shear and bulk moduli $G = 40{,}000$ Pa and $K = 100{,}000$ Pa are always the stiffest of the three phases.

Assuming a hexagonal array arrangement of the coated fibers, Fisher and Brinson (2001) calculated—with a unit cell similar to the FE-HEX one used by Brinson and Lin (1998)—the complex transverse tensile modulus $E_2^*(\omega)$ of both composites. To this end, two sets of boundary conditions had to be considered: one set in order to compute the shear modulus $G_{12}^*(\omega)$ and another for the transverse plane strain tensile modulus $E_{12,2}^*(\omega)$. The complex transverse tensile modulus is finally obtained as:

$$E_2^*(\omega) = 4G_{12}^*(\omega)\left(1 - \frac{G_{12}^*(\omega)}{E_{12,2}^*(\omega)}\right). \tag{37}$$

Fisher and Brinson (2001) also made numerical simulations with the generalized M–T scheme. The corresponding results are labeled Mori–Tanaka (three phases) in Figs. 13–16. As briefly exposed in Section 4, the same scheme could be applicable if the interface material were not coating the inclusions. Therefore we used a two-step M–T/Voigt procedure labeled two-step (M–T, Voigt) in Figs. 13–16. Taking the FE predictions as reference, the simulations show that in case of soft matrix and a stiff interphase the predictions of both homogenization methods (direct M–T and two-step M–T/Voigt) match perfectly the FE-HEX ones (Figs. 13 and 14). On the contrary, it is clearly not true if the phases' materials are switched (Figs. 15 and 16): neither the direct extension of M–T nor the two-step scheme (M–T, Voigt) shows a behavior comparable to the one of the unit cell.

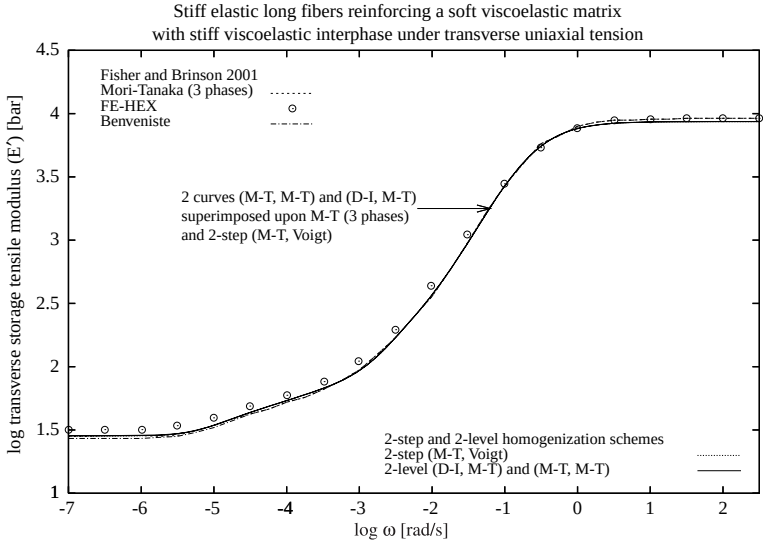

Fig. 13. Transverse storage tensile modulus as a function of frequency of a coated elastic long fiber composite. The bulk and shear moduli of the coatings and matrix phases are expanded in Prony series. Comparison between various predictive methods.

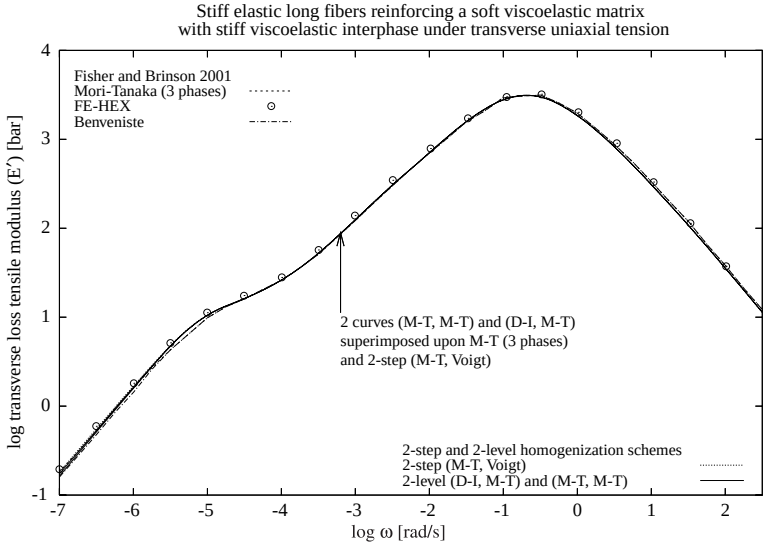

Fig. 14. Transverse loss tensile modulus as a function of frequency of a coated elastic long fiber composite. The bulk and shear moduli of the coatings and matrix phases are expanded in Prony series. Comparison between various predictive methods.

Another method to evaluate the effective behavior of three phase composites with coated inclusions is the one by Benveniste et al. (1989). The model assumes that "(...) the strain field in each part of the reinforcement phases f or g (...) are assumed to be equal to the fields in a single inclusion of phase f or g which is embedded in an unbounded matrix medium (...) and subjected to remotely applied strains (...) which are equal to the yet unknown average strain in the matrix". Although this assumption is nothing else than thinking the coatings as a separate phase combined to a M–T interpretation, this is not the generalized

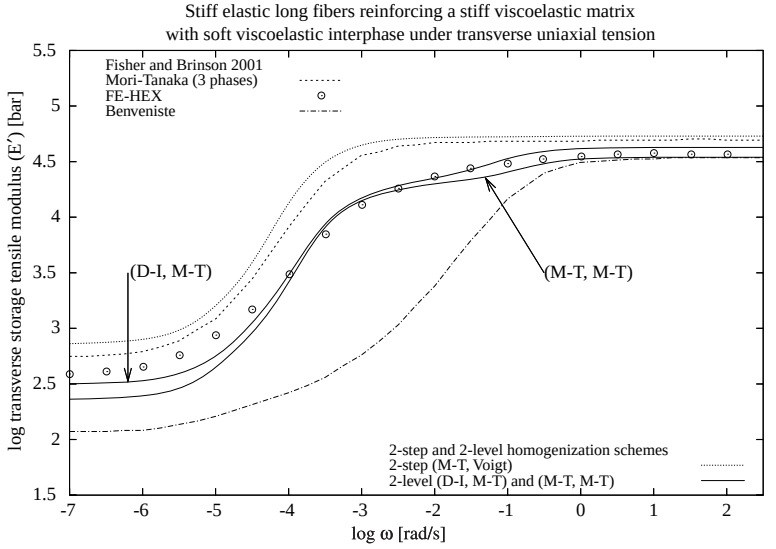

Fig. 15. Transverse storage tensile modulus as a function of frequency of a coated elastic long fiber composite. The bulk and shear moduli of the coatings and matrix phases are expanded in Prony series. Comparison between various predictive methods.

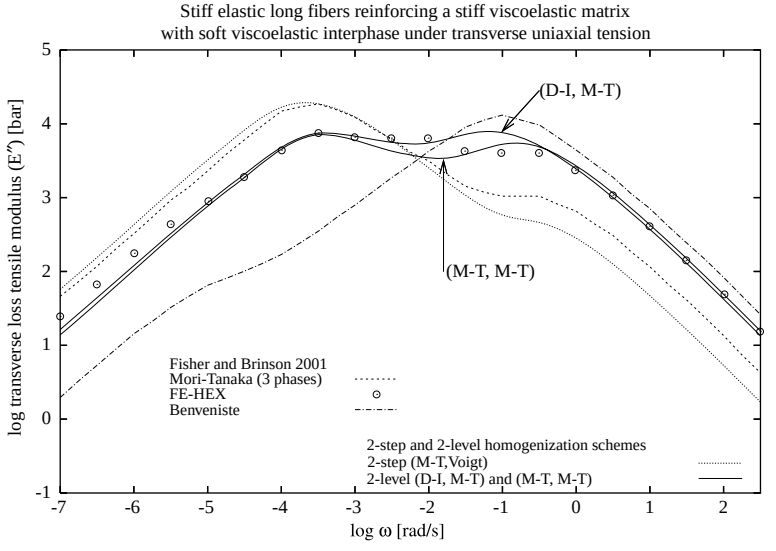

Fig. 16. Transverse loss tensile modulus as a function of frequency of a coated elastic long fiber composite. The bulk and shear moduli of the coatings and matrix phases are expanded in Prony series. Comparison between various predictive methods.

M–T scheme. The difference lies in the computation of the concentration tensors which link average strains or stresses in the reinforcement phases to the corresponding averages in the matrix. Without going into details, the model by Benveniste et al. approximates these tensors "(...) by those found when the coated inclusion is embedded in an unbounded matrix medium subjected to the average matrix stresses (or strains) at infinity". By solving average stresses and strains on a set of auxiliary problems—each problem is defined by

the (simple) loading applied at infinity—expressions for the concentration tensors are found. Compared to the generalized M–T scheme—for which the tensors are computed with help of Eshelby's result—this model is strongly limited by the geometry. Actually, Benveniste et al. (1989) presented their model for aligned coated long fibers only. With help of the elastic-viscoelastic correspondence principle, Fisher and Brinson (2001) applied the method of Benveniste et al. (1989) to predict the complex transverse tensile modulus of their two materials. Again, remarkable results are obtained for the stiff interphase composite (Figs. 13, 14) while the overall behavior is missed completely in the case of soft coatings (Figs. 15 and 16).

We made numerical simulations with our two-level homogenization approach taking M–T or interpolative D–I for the deepest level and M–T for the highest (Fig. 2). The corresponding labels are two-level (M–T, M–T) and two-level (D–I, M–T), respectively. Our predictions are confronted to all other results on Figs. 13–16. The complex transverse tensile modulus is still very well predicted in the case of a stiff coating (Figs. 13 and 14) and, unlike the other homogenization schemes, this new recursive method gives results that show good agreement with the FE-HEX ones when the interphase is made of the soft material (Figs. 15 and 16). One also observes that using the interpolative model for the deepest level leads to slightly better estimates.

6.2.2. Epoxy and copolymer matrix materials reinforced with coated ceramic particles

Marra et al. (1999) modified their original FE model by adding a viscoelastic layer that surrounds each inclusion. The idea they followed was that "energy losses likely occur at or near the interface of the ceramic and the matrix". The inclusion and matrix materials are those of Table 2. The interphase's properties are those of the matrix except its Young's loss modulus which is α times higher. The volume fraction of the layer v_i is linked to the one of the particles v_p through the relation $v_i = v_p f/(1-f)$ for a given constant f. The results they obtained with this model are labeled FE model with interphase in Figs. 17–20. The values of the two additional unknowns, α and f, were determined by fitting the predictions on the experimental points, which explains the remarkable agreement.

Taking the same values as Marra et al. (1999) for the new parameters, we used three-phase homogenization models to predict the complex tensile moduli of both composites. In each case (Figs. 17–20), our

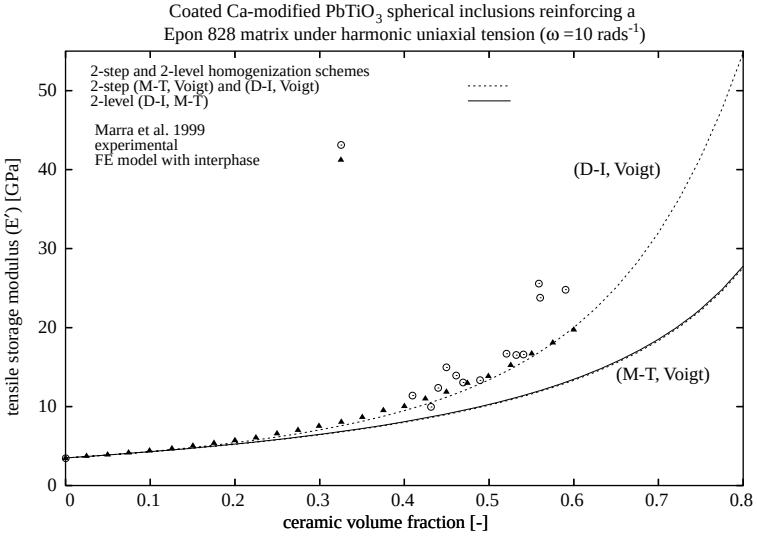

Fig. 17. Storage tensile modulus versus volume fraction of inclusions of a coated ceramic elastic particle reinforced Epon 828 viscoelastic matrix. Comparison between experiments and three-phase numerical models: FE calculations and various homogenization schemes.

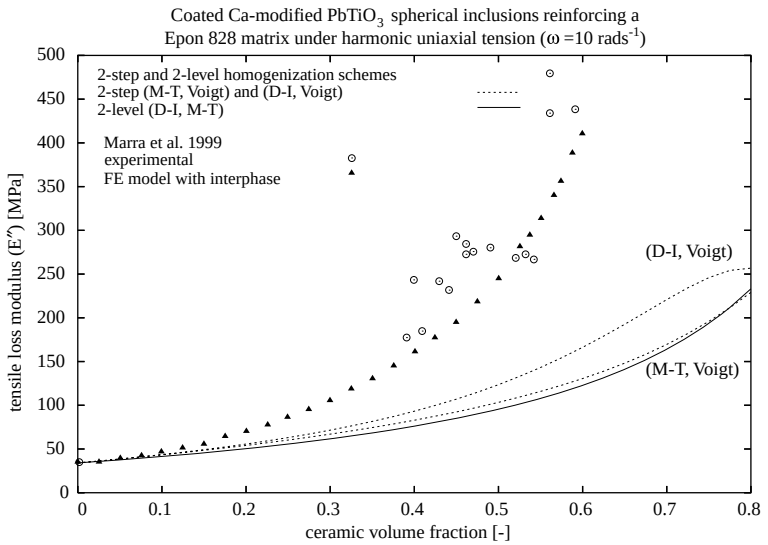

Fig. 18. Loss tensile modulus versus volume fraction of inclusions of a coated ceramic elastic particle reinforced Epon 828 viscoelastic matrix. Comparison between experiments and three-phase numerical models: FE calculations and various homogenization schemes.

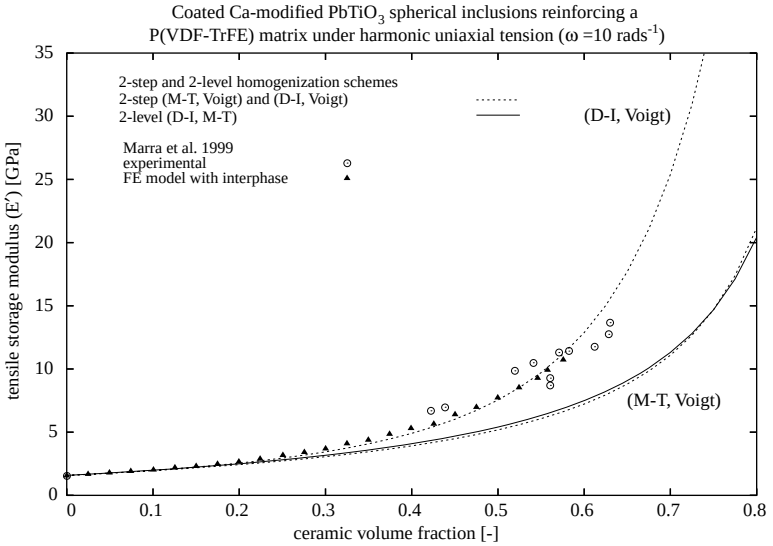

Fig. 19. Storage tensile modulus versus volume fraction of inclusions of a coated ceramic elastic particle reinforced P(VDF-TrFE) viscoelastic matrix. Comparison between experiments and three-phase numerical models: FE calculations and various homogenization schemes.

two-level scheme (D–I, M–T) underestimates the FE response and its predictions are always close to the two-step (M–T, Voigt) ones. The high volume fraction of ceramic particles (coated or not) the M–T model has to deal with explains these trends. The two-step (D–I, Voigt) works on the contrary pretty well for the storage moduli of both composites (Figs. 17 and 19). The loss moduli however are not as well estimated, especially for the reinforced epoxy matrix (Fig. 18). In comparison with the case of the copolymer matrix

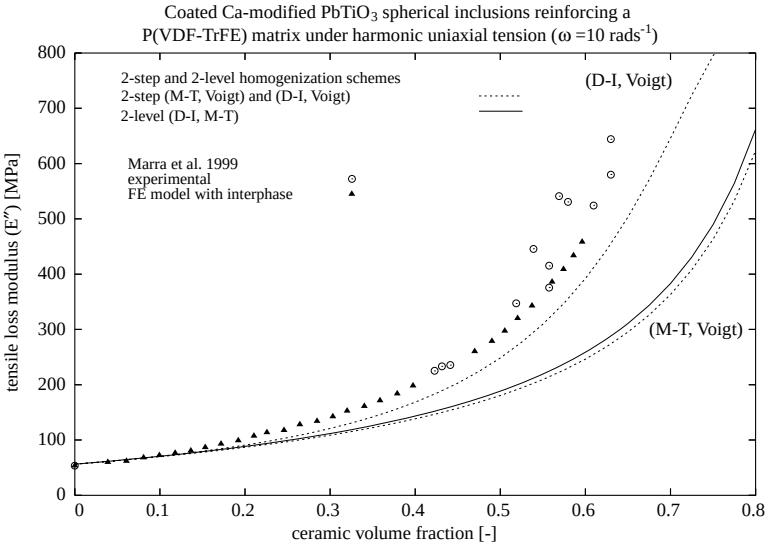

Fig. 20. Loss tensile modulus versus volume fraction of inclusions of a coated ceramic elastic particle reinforced P(VDF-TrFE) viscoelastic matrix. Comparison between experiments and three-phase numerical models: FE calculations and various homogenization schemes.

($f = 0.1, \alpha = 2$) the contrast between the loss moduli is much more pronounced ($\alpha = 33$) and the layer is much thinner ($f = 0.02$). This is a severe situation. The two-level model might overcome it if used with the interpolative D–I scheme also at the highest level. This requires the extension to the complex plane of Eshelby's tensor formulae for an inclusion in a transversely isotropic matrix (see Withers, 1989). This will be investigated in a future work.

6.3. Time behavior of two-phase viscoelastic composites

The materials hereafter should be qualified as academic since neither the composites nor the homogeneous components attempt to represent any existing material. They were actually picked up by Yi et al. (1998) who chose them to illustrate their "(...) systematic way of obtaining the effective viscoelastic moduli in time and frequency domain (...) for viscoelastic composites with periodic microstructure". The latter methodology is in form not much different from what we do: compute the effective complex moduli in a transformed domain (Laplace or Laplace–Carson) and invert them numerically into time domain. However, while both numerical inversion tools are almost indentical, the micro–macro transitions are drastically different. Assuming a periodic microstructure Yi et al. (1998) use FE unit cell calculations (in the transformed domain) in order to predict the effective moduli, while our estimates are computed by Eshelby-based mean field homogenization schemes.

Various two-phase composites are examined here. Each of them consists of elastic or viscoelastic long fibers embedded in a viscoelastic matrix (detailed material compositions are to be found on Figs. 21–23). Transverse uniaxial loading under plane strain conditions is assumed.

Our numerical simulations have been conducted with the interpolative D–I model due to the high volume fraction of fibers. As explained in Section 5 the set of collocation points should at least include the involved relaxation times, namely 1s and 10s. For these simple academic examples, they were chosen as $\theta_k = k$ for $1 \leqslant k \leqslant 10$.

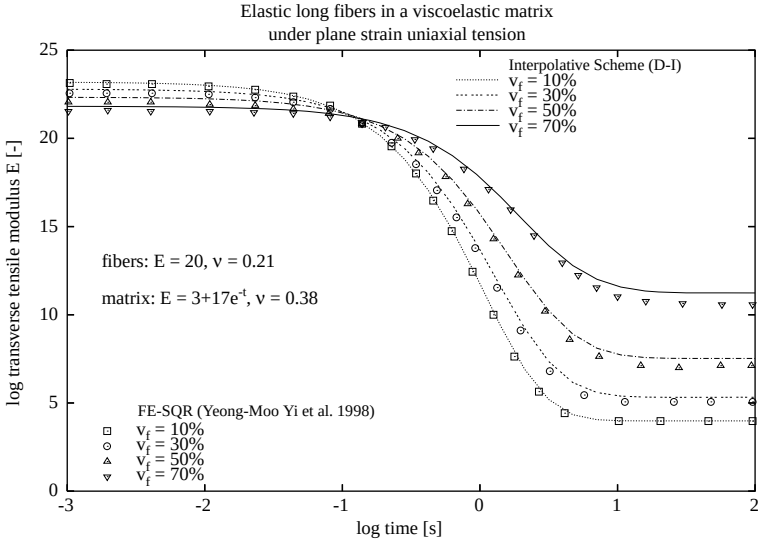

Fig. 21. Elastic long fiber reinforced viscoelastic matrix (one relaxation time). Time evolution of the plane strain transverse tensile modulus. Comparison between homogenization and finite element predictions for various volume fractions of fibers.

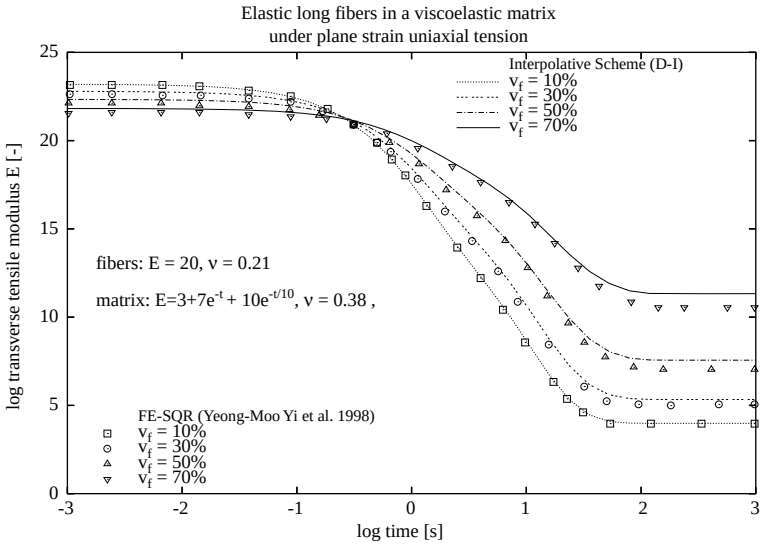

Fig. 22. Elastic long fiber reinforced viscoelastic matrix (two relaxation times). Time evolution of the plane strain transverse tensile modulus. Comparison between homogenization and finite element predictions for various volume fractions of fibers.

The predicted transverse plane strain elastic moduli are compared to those obtained by Yi et al. (1998) on Figs. 21–23. These three figures represent no less than ten distinct composites—dissimilarities lie in the concentration or in the material of the phases—and in each case both FE and D–I estimates are almost identical. This is very satisfying although these two models do not refer to the same microstructure. A periodic unit cell used in FE simulations can indeed be a good approximation of randomly distributed

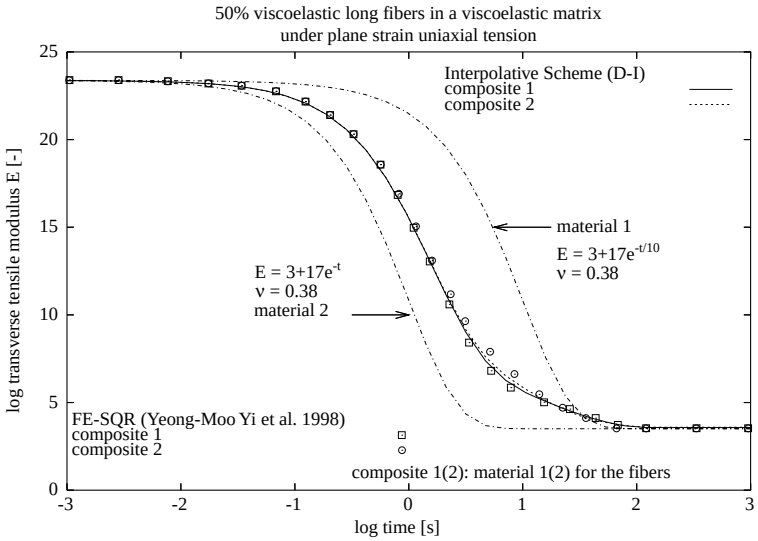

Fig. 23. Long fiber composite made of two viscoelastic materials. Time evolution of the plane strain transverse tensile modulus. Comparison between homogenization and finite element predictions for both phase configurations.

inclusions (assumed by mean-field homogenization) for linear elastic composites, but not always for non-linear composites (see Adams, 1970; Jansson, 1992; Weissenbek et al., 1994; Böhm and Han, 2001; Segurado et al., 2002; Ji and Wang, 2003; Saraev and Schmauder, 2003; Carrere et al., 2004; Iwamoto, 2004). Due to the elastic-viscoelastic correspondence principle, the good agreement between FE simulations and D–I estimates can be considered in our case as a validation. However, in order to be have a complete validation, comparisons should be made with FE calculations conducted on RVEs (not unit cells) containing a random distribution of the fibers. These more realistic FE simulations are very expensive in regard to the CPU and user times which both are already high in the case of periodic microstructures. Remember that in the FE analyses for each fiber volume fraction (here five in total) a new FE mesh has to be built. On the contrary, only a change in the value of a single parameter is needed for the interpolative scheme. Moreover, homogenization models provide a three dimensional response: the output is a tensor from which the moduli are extracted. With the FE based method, new analyses, numerical inversions and sometimes new meshes would be necessary if we were interested in other moduli.

7. Conclusions

In this paper, we presented general schemes for the mean-field homogenization in the linear visco-elastic regime of matrix materials reinforced with multiple phases of ellipsoidal inclusions, either coated or not.

A general two-step homogenization procedure suitable for multi-phase composites was extended from linear elasticity to linear viscoelasticity. For composites with coated inclusions, we proposed two general methods: two-step and two-level schemes. We compared them mathematically to a commonly used direct M–T method. For a two-phase composite, either standalone or arising from two-step or two-level homogenization schemes, we recommend using a viscoelastic version of Lielens (1999) interpolative scheme based on Nemat-Nasser and Hori (1999) D–I models. The scheme is an analytical but non-trivial interpolation between M–T and inverse M–T estimates.

We put a special emphasis on an extensive validation of the proposed methods against available experimental data and unit cell FE results. We tried severe cases (high volume fractions of inclusions, high contrasts between materials properties, soft or stiff matrices).

For two-phase composites, several simulations were presented in the frequency domain (Figs. 5–12). As compared to reference unit cell FE results, the predictions of the interpolative D–I model were always excellent and better than those of M–T for high volume fractions of inclusions (see Figs. 7–12).

The same remarkable predictions of interpolative D–I were also observed in the time domain (Figs. 21–23).

For composites with coated inclusions, the numerical simulations (see Figs. 13–20) show that in each case our proposed two-level or two-step schemes, or both of them give excellent predictions, except in one instance (Fig. 18). For stiff fibers coated with a soft viscoelastic layer and embedded in a stiff viscoelastic matrix, our proposed schemes performed remarkably well while two other methods, namely a direct M–T and Benveniste et al. (1989) procedure gave very wrong estimates (Figs. 15 and 16).

There are at least a few directions for future work. One issue is to better assess the predictive capabilities and limitations of the proposed two-step and two-level schemes for coated composites. For instance, in Figs. 15 and 16, the predictions of the two-level scheme are truly remarkable and much better than those of the two-step scheme, a direct M–T method or the model of Benveniste et al. (1989). However, in Figs. 17, 19 and 20, the two-step interpolative D–I/Voigt procedure performed much better than the two-level scheme. Finally, for the same coated composite, while the prediction of the storage modulus by the two-step interpolative D–I/Voigt is excellent (Fig. 17), that of the loss modulus is very poor (Fig. 18).

Another subject for future work is to extend the proposed methods to nonlinear viscoelasticity, perhaps by using the so-called affine formulation, which was developed successfully for elasto-viscoplasticity (e.g. Masson, 1998; Pierard and Doghri, 2004).

Acknowledgements

We would like to thank Mr. Olivier Pierard and Mr. Amine Ouaar for their help in the preparation of this manuscript. We gratefully acknowledge the support of the Belgian Federal Science Policy, IUAP P5/08 project. ''From microstructure towards plastic behavior of single- and multi-phase materials'', and Région Wallonne through SIVA Project ''Numerical Simulation of Acoustic Problems'' (991/4287) and the WINNOMAT Program (Contract 415660).

References

Aboutajeddine, A., Neale, K.W., 2005. The double-inclusion: a new formulation and new estimates. Mechanics of Materials 37, 331–341.

Adams, D.F., 1970. Inelastic analysis of a unidirectional composite subjected to transverse normal loading. Journal of Composite Materials 4, 310–328.

Benveniste, Y., 1987. A new approach to the application of Mori–Tanaka's theory in composite materials. Mechanics of Materials 6, 147–157.

Benveniste, Y., Dvorak, G.J., Chen, T., 1989. Stress fields in composites with coated inclusions. Mechanics of Materials 7 (4), 305–317.

Benveniste, Y., Dvorak, G.J., Chen, T., 1991. On diagonal and elastic symmetry of the approximate effective stiffness tensor of heterogeneous media. Journal of the Mechanics and Physics of Solids 37 (7), 927–946.

Böhm, H.J., Han, W., 2001. Comparisons between three-dimensional and two-dimensional multi-particle unit cell models for particle reinforced metal matrix composites. Modelling and Simulation in Materials Science and Engineering 9, 47–65.

Brinson, L.C., Lin, W.S., 1998. Comparison of micromechanics methods for effective properties of multiphase viscoelastic composites. Composite Structures 41, 353–367.

Camacho, C.W., Tucker III, C.L., Yalvac, S., McGee, R.L., 1990. Stiffness and thermal expansion predictions for hybrid short fiber composites. Polymer Composites 11 (4), 229–239.

Carrere, N., Valle, R., Bretheau, T., Chaboche, J.-L., 2004. Multiscale analysis of the transverse properties of Ti-based matrix composites reinforced by SiC fibres: from the grain scale to the macroscopic scale. International Journal of Plasticity 20 (4/5), 783–810.

Chabert, E., Dendievel, R., Gauthier, C., Cavaillé, J.-Y., 2004. Prediction of the elastic response of polymer based nanocomposites: a mean field approach and a discrete simulation. Composites Science and Technology 64, 309–316.

Chandra, R., Singh, S.P., Gupta, K., 2002. Micromechanical damping models for fiber-reinforced composites: a comparative study. Composites: Part A 33, 787–796.

Chazeau, L., Paillet, M., Cavaillé, J.Y., 1999. Plasticized PVC reinforced with cellulose whiskers. I. Linear viscoelastic behavior analysed through the quasi-point defect theory. Journal of Polymer Science: Part B: Polymer Physics 37, 2151–2164.

Cherkaoui, M., Muller, D., Sabar, H., Berveiller, M., 1996. Thermoelastic behavior of composites with coated reinforcements: a micromechanical approach and applications. Computational Materials Science 5, 45–52.

Christensen, R.M., 1969. Viscoelastic properties of heterogeneous media. Journal of the Mechanics and Physics of Solids 17, 23–41.

Christensen, R.M., 1992. Mechanics of Composite Materials. John Wiley and Sons, New York.

Christensen, R.M., Lo, K.H., 1979. Solutions for effective shear properties in three phase sphere and cylinder models. Journal of the Mechanics and Physics of Solids 27, 315–330.

Doghri, I., Tinel, L., 2005. Micromechanical modeling and computation of elasto-plastic materials reinforced with distributed-orientation fibers. International Journal of Plasticity 21 (10), 1919–1940.

Eshelby, J.D., 1961. Elastic inclusions and inhomogeneities. In: Sneddon, I.N., Hill, R. (Eds.), Progress in Solid Mechanics, Vol. II. North-Holland Publishing Company, Amsterdam (Chapter 3).

Fisher, F.T., Brinson, L.C., 2001. Viscoelastic interphases in polymer–matrix composites: theoretical models and finite-element analysis. Composites Science and Technology 61, 731–748.

Hashin, Z., 1962. The elastic moduli of heterogeneous materials. Journal of Applied Mechanics 29, 143–150.

Hashin, Z., 1965. Viscoelastic behavior of heterogeneous media. Journal of Applied Mechanics—Transactions of the ASME 32E, 630–663.

Hashin, Z., 1970. Complex moduli of viscoelastic composites—I. General theory and application to particulate composites. International Journal of Solids and Structures 6, 539–552.

Herve, E., Zaoui, A., 1993. *n*-Layered inclusion-based micromechanical modelling. International Journal of Engineering Science 31 (1), 1–10.

Iwamoto, T., 2004. Multiscale computational simulation of deformation behavior of TRIP steel with growth of martensitic particles in unit cell by asymptotic homogenization method. International Journal of Plasticity 20 (4/5), 841–869.

Jansson, S., 1992. Homogenized nonlinear constitutive properties and local stress concentration for composites with periodic internal structure. International Journal of Solids and Structures 29 (17), 2181–2200.

Ji, B., Wang, T., 2003. Plastic constitutive behavior of short-fiber/particle reinforced composites. International Journal of Plasticity 19 (5), 565–581.

Lielens, G., 1999. Micro–Macro Modeling of Structured Materials. PhD thesis, Université Catholique de Louvain, Belgium.

Marra, S.P., Ramesh, K.T., Douglas, A.S., 1999. The mechanical properties of lead-titanate/polymer 0–3 composites. Composites Science and Technology 59, 2163–2173.

Masson, R., 1998. Estimations non linéaires du comportement global de matériaux hétérogènes en formulation affine. PhD thesis, Ecole Polytechnique, France.

Mori, T., Tanaka, K., 1973. Average stress in matrix and average elastic energy of materials with misfitting inclusions. Acta Metallica 21, 571–574.

Mura, T., 1987. Micromechanics of Defects in Solids, second revised ed. Martinus Nijhoff Publishers, Dordrecht, The Netherlands.

Nemat-Nasser, S., Hori, M., 1999. Micromechanics: Overall Properties of Heterogeneous Materials, second ed. Elsevier Science Publishers, Amsterdam.

Pierard, O., Friebel, C., Doghri, I., 2004. Mean-field homogenization of multi-phase thermo-elastic composites: a general framework and its validation. Composites Science and Technology 64, 1587–1603.

Pierard, O., Doghri, I., 2004. An enhanced affine formulation and the corresponding numerical algorithms for the mean-field homogenization of elasto-viscoplastic composites. Submitted to International Journal of Plasticity.

Redaelli, S., 2002. Damping Properties of Polymeric Materials. PhD thesis, Politecnico di Milano, Italy.

Saraev, D., Schmauder, S., 2003. Finite element modeling of Al/SiCp metal matrix composites with particles aligned in stripes- a 2D–3D comparison. International Journal of Plasticity 19 (6), 733–747.

Sarvestani, A.S., 2003. On the overall moduli of composites with spherical coated fillers. International Journal of Solids and Structures 40, 7553–7566.

Schapery, R.A., 1962. Approximate methods of transform inversion in viscoelastic stress analysis. In: Proceedings of the Fourth US National Congress on Applied Mechanics. ASME, pp. 1075–1085.

Segurado, J., Llorca, J., Gonzalez, C., 2002. On the accuracy of mean-field approaches to simulate the plastic deformation of composites. Scripta Materialia 46, 525–529.

Weissenbek, E., Böhm, H.J., Rammerstorfer, F.G., 1994. Micromechanical investigations of arrangement effects in particle reinforced metal matrix composites. Computational Materials Science 3, 263–278.

Wineman, A.S., Rajagopal, K.R., 2000. Mechanical Response of Polymers: An Introduction. Cambridge University Press.

Withers, P.J., 1989. The determination of the elastic field of an ellipsoidal inclusion in a transversely isotropic medium, and its relevance to composite materials. Philosophical Magazine A 59, 759–781.

Yi, Y.-M., Park, S.-H., Youn, S.-K., 1998. Asymptotic homogenization of viscoelastic composites with periodic microstructures. International Journal of Solids and Structures 35 (17), 2039–2055.